Research Article

Mathematical Methods in the Applied Sciences

Received 4 May 2013

Published online 16 January 2014 in Wiley Online Library

(wileyonlinelibrary.com) DOI: 10.1002/mma.3007
MOS subject classification: 35 A 9;35 G 46

Mathematical modeling of drug delivery from cylindrical implantable devices

Juan C. D. Ibarra*†, Ignacio M. Helbling and Julio A. Luna

Communicated by G. Ding

A mechanistic mathematical model applicable to the controlled dispersed-drug release from cylindrical device such as implantable drug delivery system was derived. Analytical solutions based on the pseudosteady state approximation are derived taken account an exact external medium volume. The model prediction is accurate when the initial drug load is higher than the drug solubility in the polymer. The results obtained are compared with the analytical solutions available in the literature. The equations are corroborated by comparison with experimental profiles reported in the literature for sink conditions and non sink conditions. The evolution of concentration distribution profiles is compared for different volume of external medium. A reduction in the volume of the external solution leads to an increase in the concentration on the surface of the device, which determines decreases in the release of drug. One criterion for determining whether the volume of external solution should be considered for the prediction of drug release from cylindrical devices is established. This criterion is based on establishing a maximum percentage error allowed in the values of amount of drug released. The usefulness of the model is focused in the design of implant for controlled release of drug into a small volume of external medium of release.

Keywords: cylindrical geometry; partial differential equations; controlled release; implant; finite external medium

1. Introduction

In the area of pharmacology treatments, some therapies require that the drug be repeatedly administered to the patient over a long period. The development of controlled drug release from implantable device has been a response to these situations. The implantable drug delivery system (IDDS) has been designed to release drugs within the body and thereby avoid the periodic insertion of the drug by other routes of administration (oral, parenteral, transdermal, etc.). The use of IDDS decreases number of dosage and generates a less invasive dosing, leading to improved patient compliance [1, 2]. The IDDSs have been applied in numerous areas of medical treatment including diabetes, cancer, contraception, cardiovascular diseases, and brain diseases among others [3–5].

The mathematical models to describe the kinetics of release from polymeric systems loaded with drugs have been a subject of practical importance in designing of IDDS. The development of new mechanistic mathematical models for IDDS logically must consider the specifics of this type of systems. The monolithic matrix is the most common of the devices for controlling the release from IDDS because of the ease in their manufacture, low probability of high doses dangerous for the patient, among other advantages [6]. Another distinctive feature of these systems is attached to the need for a dosage form small and/or a release of drug for an extended period. In these cases, the initial load of drug (A) should be set above the solubility of the drug in the matrix (C_S). This leads to the existence of drug particles dispersed in the matrix. If the diffusion of the drug is slower than the dissolution of the drug, the release process will be controlled by the diffusion of the drug to the external medium, according with the Fick's laws [7]. The mathematical description of this type of mass transfer problems are known as moving boundary problems [8] and are applicable to the release from IDDS matrix type with load of drug above the solubility in the matrix.

The in vitro release tests are designed depending on the subsequent use of the drug delivery device in vivo. For example, for devices that will be used in vivo in small volumes of fluids or fluids with very low solubility of the drug, the in vitro release tests should be performed in finite volume of the external medium. The exact value of external volume is an important parameter to simulate the in vivo condition. This in vitro test condition, allows the analysis of the phenomenon of partition as controlling mechanism of drug release.

Laboratorio de Química Fina, Instituto de Desarrollo Tecnológico para la Industria Química (INTEC), Universidad Nacional del Litoral and Consejo Nacional de Investigaciones Científicas y Técnicas (UNL-CONICET), Centro Científico Tecnológico, Ruta Nacional 168, Paraje El Pozo 3000, Santa Fe, Argentina

**Correspondence to: Juan C. D. Ibarra, Laboratorio de Química Fina, Instituto de Desarrollo Tecnológico para la Industria Química (INTEC), Universidad Nacional del Litoral and Consejo Nacional de Investigaciones Científicas y Técnicas (UNL-CONICET), Centro Científico Tecnológico, Ruta Nacional 168, Paraje El Pozo 3000, Santa Fe, Argentina.*

† E-mail: jcdibarra@santafe-conicet.gov.ar

The controlled drug release in periodontal pockets [9], eyes [10, 11], bones [12], and gastrointestinal tract [13] is usually performed in this condition. The mathematical models used for the prediction of the release of drug in these in vitro release systems cannot assume sink conditions. The addition of the exact volume of the external medium as a parameter can be an important tool depending on the site of implantation in vivo of the drug release device.

The design of the IDDS is generally of cylindrical geometry because of the implantation of the devices is performed with the use of needles. The implantation of devices for estrous cycle control in animals is performed with guns with needles at the tip, and the implantation of devices for contraception in women is performed with specially designed needles, to mention some examples [14, 15]. The mathematical modeling of drug release from a cylindrical matrix has been extensively described but has not been possibly an explicit analytical solution because of the complexity of partial differential equations. Roseman and Higuchi developed a model for dispersed-drug systems using the pseudosteady state assumption (PSSA) and taking into account the presence of a diffusion boundary layer under sink conditions [16]. Zhou derived solutions for dispersed-drug release from a two-dimensional cylindrical matrix in a perfect sink [17]. Analytical solutions for cylindrical systems that assume specific conditions of release such as a finite external medium can be obtained with the use of the PSSA. This approximation has been used previously to incorporate the phenomenon of finite external medium in basic geometries such as slab and sphere [18–20]. However, to apply the solution obtained, the delivery system must fulfill all the assumptions in order to establish that the release mechanism is similar to the mechanism studied by Higuchi [21, 22]. The PSSA yields satisfactory results for the cases in which $A/C_S \geq 3$ [16–23]. The purpose of the present work was to derive a mathematical model to predict of controlled release of drug from IDDS cylindrical matrix type with initial drug loading higher than the maximum solubility of drug in the polymer, assuming PSSA and taking into account the existence of finite volume of external medium.

2. Model development

2.1. Theoretical consideration

The mathematical model is developed for cylindrical single-layer devices containing solid drug particles. The system is illustrated in Figure 1. The assumptions of the model are the following: (i) the system is a cylindrical single-layer device; (ii) the device is composed by a polymeric matrix that contain solid drug particles dispersed because the initial drug loading in the matrix is higher than the maximum drug solubility in the polymer; (iii) the device is considered as an isotropic medium; (iv) the polymeric matrix is inert, unswellable, and nonerodible; (v) the initial drug distribution is homogeneous in the polymeric matrix; (vi) the rate controlling step of the release process is the drug diffusion across the polymeric matrix, which is described according to Fick's laws; (vii) the mass transport of drug is assumed to be effectively one-dimensional; (viii) the drug diffusion coefficient in the polymeric matrix is considered constant; (ix) resistance to external mass transfer is negligible; (x) the volume of the external medium (V) is considered finite; (xi) the pseudosteady state approximation (PSSA) is assumed during the whole modeling process; (xii) there exist a drug depletion zone with a thickness $L = R\text{-}S(t)$. This thickness increases with time of the release, thus leading to the inward advancement of the interface of the dispersed-drug zone/depleted drug zone, phenomenon referred to as 'dissolution–diffusion moving front' (xiii) the model formulated is valid till all solid drug particles dissolve in the polymer; and (xiv) at the initial time ($t = 0$), there is no depletion zone because the external medium is not in contact with the dispersed drug.

The general diffusion equation describing the concentration distribution C in the dissolved drug zone of the cylindrical matrix after exposing it to an external medium is [24]

$$\frac{\partial C}{\partial t} = D_p \frac{1}{r} \frac{\partial C}{\partial r} \left(r \frac{\partial C}{\partial r} \right) \quad S \leq r \leq R \tag{1}$$

where C is the concentration of dissolved drug in the matrix, t is the time, D_p is the drug diffusion coefficient in matrix, r is the coordinate along the matrix thickness, S is the position of the dissolution–diffusion moving front, and R is matrix thickness.

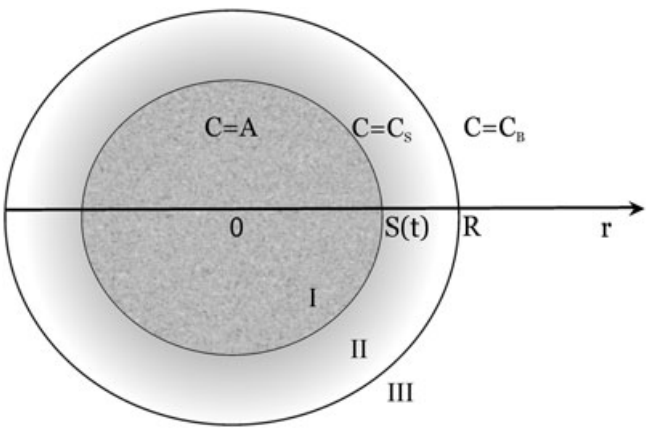

Figure 1. Schematic illustration of cylindrical single-layer devices. I, dispersed drug zone; II, dissolved drug zone; and III, finite release medium.

Practically, the release kinetics can be described by a one-dimensional model when the height to the diameter ratio is greater than 5, with an error within the experimental error [25]. Assuming equilibrium between the surface and the external fluid at all t, the initial and boundary conditions are

$$C(S,t) = C_S \tag{2}$$

$$C(R,t) = C_S{}' = \frac{C_B}{k_p} \tag{3}$$

$$S(t=0) = R \tag{4}$$

where C_S is maximum solubility of drug in the polymer, $C_S{}'$ is the drug concentration in matrix at the matrix-external medium interface, C_B is the drug concentration in the external medium and k_p is the drug partition coefficient at the matrix-external medium interface. Hereinafter, the partition coefficient will be considered equal to (1), so $C_S{}' = C_B$. With $\partial C/\partial t$ in Equation (1) being fixed at zero, according to the PSSA, and the boundary conditions presented in Equations (2)–(4), the concentration distribution in the dissolved drug zone can be derived as

$$C = C_S - \frac{(C_B - C_S)\ln(r/S)}{\ln(S/R)} \quad S(t) \leq r \leq R \tag{5}$$

This expression of concentration in the dissolved drug zone is different to the expression obtained by other authors because of the difference in the resolution of Equation (1). Taking into account the amount of dissolved drug present in the cylindrical matrix ($C \leq C_S$), the cumulative amount of drug released from the device is calculated from a mass balance equation (per unit height if $h = 1$) [17]:

$$M_t = A\pi h\left(R^2 - S^2\right) - 2\pi h\int_S^R C\, r\, dr \tag{6}$$

where h is the height of the cylinder. Substituting Equation (5) in Equation (6) and integrating respect to r with S and R as the integration limits, the amount of solute released in a given time results in

$$M_t = (A - C_S)\pi h\left(R^2 - S^2\right) - \frac{(C_B - C_S)\pi h}{\ln(S/R)}\left[R^2\ln(S/R) + \left(\frac{R^2 - S^2}{2}\right)\right] \tag{7}$$

The amount of solute released can be obtained from Equation (7). To use Equation (7), the values of S and C_B must be determined. The values of C_B can be calculated in the following manner. The drug concentration in the external medium (C_B) can be expressed as the amount of solute released (M_t) divided by the volume of external medium (V). Dividing both terms of Equation (7) by V, remembering that $C_B = M_t/V$, rearranging and solving for C_B, the following expression can be obtained:

$$C_B = \frac{G_1 k_p}{b} \tag{8}$$

where

$$G_1 = \left(R^2 - S^2\right)(A - C_S) + C_S R^2 + \frac{C_S\left(R^2 - S^2\right)}{2\ln(S/R)} \tag{9}$$

$$b = k_p\left[\frac{R^2}{k_p} + \left[\frac{\left(R^2 - S^2\right)}{2k_p\ln(S/R)}\right] + \frac{V}{\pi h}\right] \tag{10}$$

According to Fick's law, the rate of solute release from cylindrical surface area in the dissolution–diffusion moving front can be written as

$$\frac{dM_t}{dt} = -2\pi h S D_p\left(\frac{dC}{dr}\right)_S \tag{11}$$

The concentration distribution in dissolved drug zone obtained using Equation (5) has a logarithmic form. A schematic illustration of a logarithmic profile in the depletion zone of a cylindrical device is presented in Figure 2.

2.2. *General solutions*

The amount of solute released can be obtained from Equation (7). To use Equation (7), it is necessary to know the values of S for each time point considered. Differentiating Equation (7) with respect to S leads to:

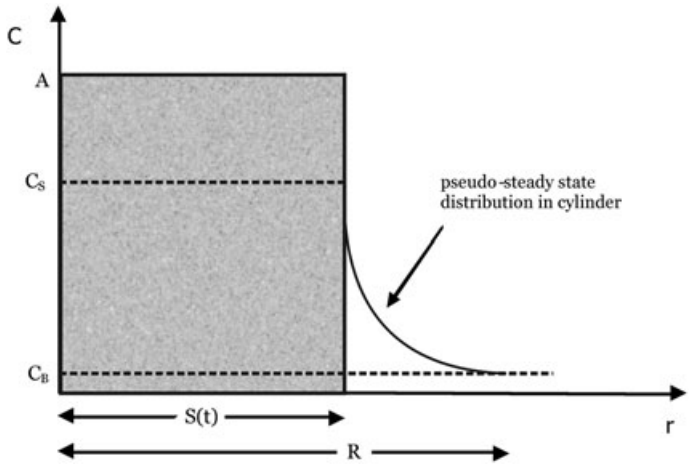

Figure 2. Schematic illustration of a logarithmic concentration profiles in the polymeric device.

$$\frac{dM_t}{dS} = \frac{2V_m}{R}\left(A + \frac{G_1}{b}\right) - \left\{\left[V_m + \frac{\pi h\left(R^2 - S^2\right)}{2\ln\left(S/R\right)}\right]\left(\frac{G_2}{b} - \frac{G_3 G_1}{b^2}\right)\right\} + \frac{\left[V_m \ln\left(S/R\right) + \frac{\pi h\left(R^2 - S^2\right)}{2}\right]\left(C_S - \frac{G_1}{b}\right)}{R\left[\ln\left(S/R\right)\right]^2} \tag{12}$$

where V_m is the volume matrix defined as

$$V_m = \pi h R^2 \tag{13}$$

$$G_2 = 2AR + \frac{C_S R}{\ln\left(S/R\right)} + \frac{C_S\left(R^2 - S^2\right)}{2R\left[\ln\left(S/R\right)\right]^2} \tag{14}$$

$$G_3 = \left[2R + \frac{R}{\ln\left(S/R\right)} + \frac{\left(R^2 - S^2\right)}{2R\left[\ln\left(S/R\right)\right]^2}\right] \tag{15}$$

For all time t, the following equation must be satisfied:

$$\frac{dM_t}{dt} = \frac{dM_t}{dS}\frac{dS}{dt} \tag{16}$$

Substituting Equations (10) and (11) in Equation (16) and rearranging results in

$$dt = \left\{\begin{array}{l} \frac{2V_m}{R}\left(A + \frac{G_1}{b}\right) - \frac{V_m \ln(S/R)\left(\frac{G_2}{b} + \frac{G_3 G_1}{b^2}\right) + \frac{\left(R^2 - S^2\right)}{2}}{\ln(S/R)} + \\ \frac{\left[V_m \ln(S/R) + \frac{\pi h\left(R^2 - S^2\right)}{2}\right]\left(Cs + \frac{G_1}{b}\right)}{R[\ln(S/R)]^2} \end{array}\right\}\left[\frac{\ln\left(S/R\right)}{2\pi h D_p\left(C_B - C_S\right)}\right] dS \tag{17}$$

Integrating within the time lapse corresponding to the moving front between $[R, S]$, it yields

$$t = \frac{1}{2\pi h D_p}\int_R^{S'}\left\{\left\{\begin{array}{l} \frac{2V_m}{R}\left(A + \frac{G_1}{b}\right) - \frac{V_m \ln(S/R)\left(\frac{G_2}{b} + \frac{G_3 G_1}{b^2}\right) + \frac{\left(R^2 - S^2\right)}{2}}{\ln(S/R)} + \\ \frac{\left[V_m \ln(S/R) + \frac{\pi h\left(R^2 - S^2\right)}{2}\right]\left(C_S + \frac{G_1}{b}\right)}{R[\ln(S/R)]^2} \end{array}\right\}\left[\frac{\ln\left(S/R\right)}{\left(C_B - C_S\right)}\right]\right\} dS \tag{18}$$

No explicit solution can be obtained by integrating Equation (18). Therefore, the position of the dissolution–diffusion moving front can be obtained from Equation (18) using an adequate computational software.

The fraction of drug released (*FDR*) is defined as

$$FDR = \frac{M_t}{M_0} = \frac{M_t}{AV_m} \tag{19}$$

where M_0 is the amount of drug loaded into the device initially.

The cumulative amount of drug released per unit release area is defined as

$$Q = \frac{M_t}{2\pi Rh} \tag{20}$$

Equations (7) and (18) are valid only till the entire drug dispersed in the matrix is dissolved ($S = 0$).

3. Result and discussion

3.1. Validation with limiting cases

The model was essentially developed to predict the release of drug into a finite external medium. However, the model can also be used for the case in which $V \to \infty$. To corroborate the validity of the equations in this limiting case, a comparison of the theoretical prediction with the experimental data was performed. In addition, a comparison with the analytical solutions available in the literature for this limiting case, that is the solutions reported by Roseman and Higuchi [16], was included. The comparison was performed for both the position of the dissolution–diffusion moving front and the cumulative amount of drug released obtained from Equations (18) and (7), respectively.

The thickness of dissolved drug zone was defined as

$$L(t) = R - S(t) \tag{21}$$

The variable L represents the distance covered by the front S at each time t and determines the thickness of the dissolved drug zone within the matrix. Figure 3 presents the L values calculated from Equation (18) and the values the L calculated from the solution reported by Roseman and Higuchi for release from matrices without resistance to external mass transfer. The symbols represent the experimental data reported by these authors of the thickness of depletion zone for silicone cylindrical matrix loaded with medroxyprogesterone acetate [16]. Two systems with different initial drug loading were compared, and in both cases, $A \gg C_S$.

The parameters employed were taken from Roseman [16], including the diffusion coefficient in matrix. Also, the aspect ratio is greater than 10, which enables to use a 1D model in this case. Zhou and Wu reported that $V/V_m = 5000$ for planar case approximate $V \to \infty$ [18]. To mimic the sink condition, a value of $V/V_m > 15000$ was used as parameter in the model developed.

The experimental data show that increasing the initial drug load, the value of L for a given time t, decreases. This is an expected result because the matrix contains greater amount of drug, and therefore, the dissolution-diffusion moving front progresses more slowly. Both models fit well with experimental data within experimental error using the same parameters. However, there are differences between the values of L obtained by the model developed and the values obtained with the model reported by Roseman. These are attributed to the differences in the profiles of dissolved drug distribution in the depletion zone of both models. The results show that with Equation (18) smaller values of L are obtained in comparison with those calculated by Roseman model during the release process, except very short times. This means that the present model predicts that S is moving faster than the S predicted by the model Roseman at short times and slower than the S predicted by the model Roseman throughout the rest of the release. This behavior is observed in both initial drug loads. Increasing the initial drug load appears to decrease the difference between the predictions of both models.

The effect of the initial drug load on the L values predicted by both models was analyzed more thoroughly as follows. First, the dimensionless variable ε was defined as

$$\varepsilon(t) = \frac{S(t)}{R} \tag{22}$$

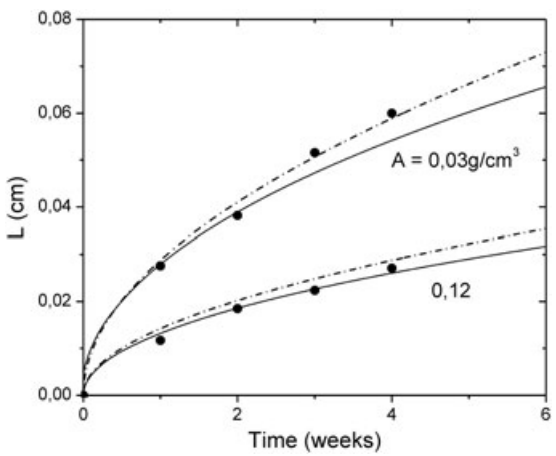

Figure 3. Comparison of thickness of dissolved drug zone calculated according to Equation (18) (—), the model reported by Roseman (···), and the experimental data (•) reported for different initial drug loading [16]. The parameters used are $R = 0.5$ cm; $h = 4$ cm; $V/V_m = 5000$; $D_p = 2.0 \times 10^{-7}$cm^2/s.

Again, the thickness of the zone of dissolved drug was defined, now in dimensionless form:

$$\delta(t) = 1 - \varepsilon(t) \tag{23}$$

The variable δ represents the distance covered by the moving front at each time t and determines the thickness of the dissolved drug zone within the matrix in the same way as to the value of L, but in dimensionless form, that is, ranging from 0–1. The difference between the values of δ predicted by both models was calculated and expressed as a percentage:

$$\text{Differences in } \delta\ (\%) = \frac{(\delta_M - \delta_R)}{\delta_R} \cdot 100 \tag{24}$$

where δ_R is the value predicted by Roseman model and δ_M is the value predicted by the present model. In this expression, the difference between the models was divided by the δ value of Roseman model because thus a more general comparison is achieved. Figure 4 shows the differences in $\delta(\%)$ versus time to the cases discussed earlier in Figure 3 and adding a smaller drug loading ($A = 0.01$ g/cm^3). The rest of the parameters were set with the same values as in Figure 3.

The model's differences show negative values at short times and positive values in the rest of the release process. At short times, the present model predicts values of $\delta(\%)$ greater than the prediction of the Roseman model. The difference decreases to zero with the time. This time t in which there is accurate similarity between models, that is, there is no difference in the predictions, was named t_s. After this time t_s, the Roseman model predicts values of $\delta(\%)$ greater than the prediction of the present model. The value of t_s is increasing with the value of the initial drug loading. In this stage, after t_s, when increasing the value of the initial drug loading, lower values of the model's differences in $\delta(\%)$ are obtained.

To complete the analysis, Figure 5 shows the profile of cumulative amount of drug released (M_t) for the delivery of medroxyprogesterone acetate from silicone cylindrical matrix for two initial drug loading reported in the literature [16]. The experimental values were compared with profiles calculated according to Equation (7) and the prediction of Roseman model.

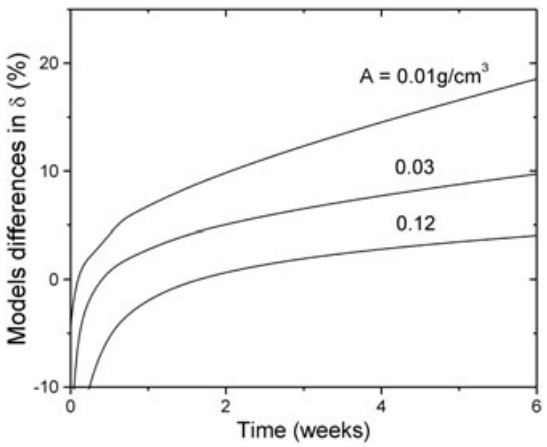

Figure 4. Differences between the present model and the Roseman model in $\delta(\%)$ versus time for different initial drug loading.

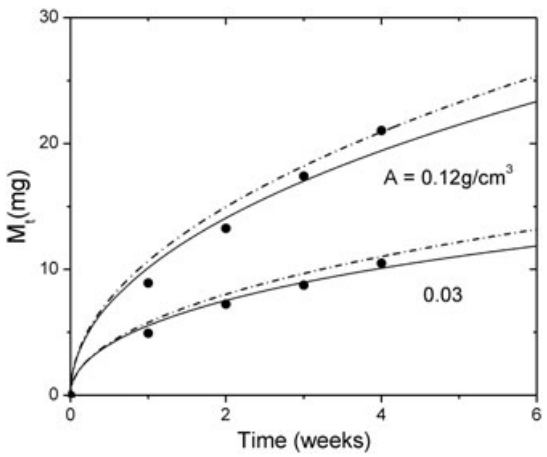

Figure 5. Comparison of the profile of cumulative amount of drug released (M_t) calculated according to Equation (7) (—), the model reported by Roseman (· · ·), and the experimental data (●) reported for different initial drug loading [16]. The parameters used are $R = 0.5$ cm; $h = 4$ cm; $V/V_m = 5000$; $D_p = 2.0 \times 10^{-7}$cm^2/s.

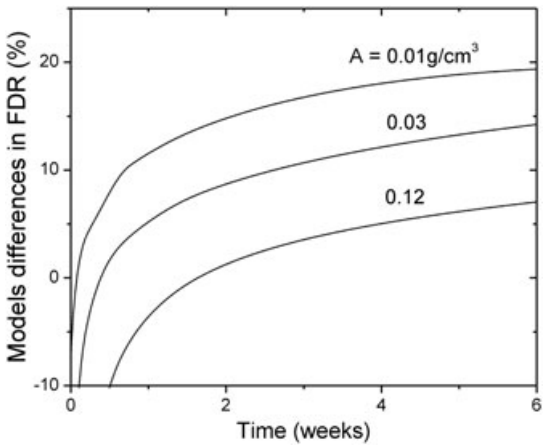

Figure 6. Differences between the present model and the Roseman model in *FDR*(%) versus time for different initial drug loading.

The experimental data show that increasing the initial drug load, the value of M_t for a given time t, increases. This is an expected result because the matrix contains larger amount of drugs, and therefore, greater amount of drug is released. The present model is in agreement with the experimental data. The excellent agreement obtained shows that the model has a wide range of usefulness in the prediction of drug release in sink conditions.

There are differences between the predictions obtained by both models. The results show that with Equation (7) smaller values of M_t are obtained in comparison with the values calculated by Roseman model during the release process, except very short times. This behavior is similar to that observed in the previous analysis of L. This result was expected because there is a direct correlation between the distance covered by the front S (values of L) and the amount of drug released at time t (M_t). This difference between the models is attributed to the differences in the profiles of dissolved drug distribution in the depletion zone of both models, as previously mentioned.

However, the present model has another difference in mathematical development regarding Roseman model. The Roseman model assumes that M_t is equal to the amount of drug initially contained in the matrix between S and R. This amount is determined mathematically by the first term of Equation (7). In contrast, the present model adds a second term to the expression of M_t, which represents the concentration of drug in the dissolved drug. This term is subtracted from the first term, generating a lower value of M_t. This means that the values of M_t predicted by the Roseman model will be higher than those predicted by this model.

The effect of the initial drug load on the M_t values predicted by both models was analyzed more thoroughly as follows. First, the *FDR* was calculated according to the Equation (19). This step transforms the values of M_t in dimensionless values, enabling most general analysis. The difference between the values of *FDR* predicted by both models was calculated and expressed as a percentage:

$$\text{Differences in } FDR(\%) = \frac{(FDR_M - FDR_R)}{FDR_R} \cdot 100 \tag{25}$$

where FDR_R is the value predicted by Roseman model and FDR_M is the value predicted by the present model. The difference between the models was divided by the *FDR* value of Roseman model because thus a more general comparison is achieved. Figure 6 shows the differences in *FDR*(%) versus time to the cases discussed earlier in Figure 5, and adding a smaller drug loading ($A = 0.01$ g/cm^3). The rest of the parameters were set with the same values as in Figure 5.

The model's differences show negative values at short times and positive values in the rest of the release process. This is an expected result because of the direct relationship between L and M_t, therefore, between δ and *FDR*. The model's differences in *FDR* reach to zero over time. The time t in which there is accurate similarity between models was named t_s. After this time t_s, the Roseman model predicts values of *FDR*(%) greater than the prediction of the present model. The value of t_s is increasing with the value of the initial drug loading. In this stage, after t_s, when increasing the value of the initial drug loading, lower values of the model's differences in *FDR*(%) are obtained.

Furthermore, it can be seen by comparing Figures 4 and 6 that the final percentages at 6 weeks of release are greater for *FDR*(%) than for δ(%). The final values for δ(%) at $t = 6$ weeks are 18,5%; 9,7%; and 4,1%, respectively. While the final values for *FDR*(%) are 19,4%; 14,2%; and 7,0%, respectively. This is an expected result because the difference in the expression of M_t, increases the difference between the models and affects only *FDR*(%).

3.2. *Validation with experimental profiles*

The second step in the validation process was to verify the ability of the models to predict real experimental drug release profiles into finite volume. This goal was achieved by a comparison of theoretical predictions with experimental data reported in the literature [26]. Figure 7 shows experimental data reported by Li *et al.* and the model predictions obtained from Equation (19) for the *FDR* into a finite medium. The values of model parameters were taken from the work of Li *et al.*, see [26]. The A/C_S ratio was equal to 3, so the PSSA can be applied. The prediction of the model is in good agreement with the experimental data.

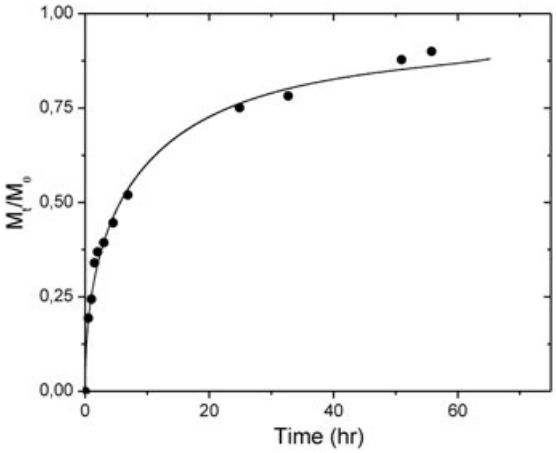

Figure 7. Comparison of the fraction of drug released calculated according to Equation (19) (—) and the experimental data (•) reported by Li (see Ref. [26]). The parameters used are $R = 0.48$ cm; $h = 1.019$ cm; $V/V_m = 35$; $D_p = 2.5276 \times 10^{-6}$cm^2/s.

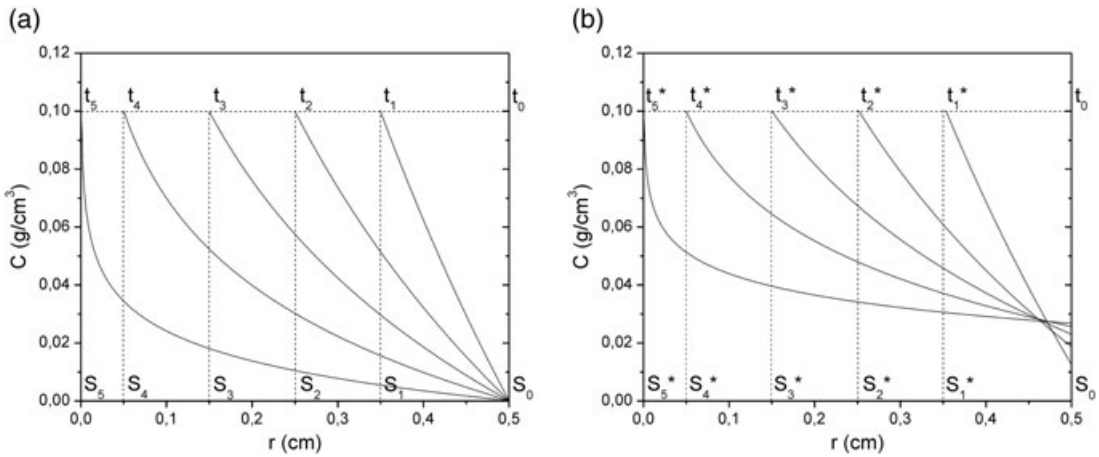

Figure 8. Concentration distribution as function of the radius of the device for different positions of the diffusion–dissolution moving front. (a) Infinite external medium and (b) finite external medium.

3.3. Effect of variation in the external medium volume

A series of simulations are presented later in order to illustrate the usefulness of the model in the analysis of controlled drug release. Figure 8 shows the profiles of concentration distribution in function of the radius of the device for different positions of the diffusion–dissolution moving front. Drug dissolved concentration profiles were plotted for different values of S_i, which correspond to different times t_i where $t_0 < t_1 < t_2 < t_3 < t_4 < t_5$. In Figure 8(a), the profile is calculated by simulating sink conditions and in Figure 8(b) using a finite volume of external solution with$V/V_m = 10$. The simulation was performed for a value of $R = 0.5$ cm and $A/C_S = 3$, where $C_S = 0.1$ g/cm^3. By reducing the volume of external solution or the V/V_m ratio, it promotes a greater concentration on the surface of the device, which determines a lower concentration gradient. By decreasing the gradient, it decreases the diffusion moving front velocity, which was confirmed because t_i^* is greater than t_i in all cases. It can be seen that in the case of finite volume of external solution, the concentration values in the external solution reach to values of 25–30% of the value of C_S. The analysis of the sink conditions with the parameter V/V_m is valid for systems while A is kept at a fixed value, that is, in a system where the same values of the parameters were kept in the simulation earlier, except the value of A, the total amount of drug in the device will have another value, despite that V_m maintains its value constant. This would determine a change in the concentration in the external solution concentration C_B on the case earlier, despite keeping the V/V_m ratio constant.

Therefore, for cases where the volume of external solution is small, it would be incorrect to consider sink conditions even though it remains perfectly agitated. To assume an external concentration equal to zero, it should be established first if the V/V_m of this specific system allows negligible concentrations in the receiver solution.

Table I shows the result of a simulation with the aim of establish a V/V_m ratio that allows assuming sink conditions. Considering $C_B < 1x10^{-4}$ g/cm^{3}as zero, the table shows that this condition is fulfilled when V/V_m is equal to 5000. This result is consistent with that established in the literature for planar case [18]. In addition, it is important to evaluate the error in the values of cumulative amount of drug released per unit area of liberation (Q) when sink condition is assumed compared with the values obtained using the real V. The 'percentage of error' is defined as the subtraction between the values predicted by the model for infinite and finite volume, divided by

Table I. Comparison of the percentage deviation from infinite volume.

V/V_m	$^*Q/C_s(D_pt)^{1/2}$	% Error	C_B(g/cm^3)
5	0.7269	−17.65	0.0482
10	0.7944	−10.01	0.0263
25	0.8427	−4.54	0.0112
100	0.8713	−1.29	0.0029
500	0.8803	−0.28	0.0006
1000	0.8815	−0.14	0.0003
3000	0.8823	−0.05	0.0001
5000	0.8824	−0.03	0.00006
8000	0.8825	−0.02	0.00004
15000	0.8826	−0.009	0.00002
Infinite volume	0.8827	—	0.00000

$^*Q$[g/cm^2]

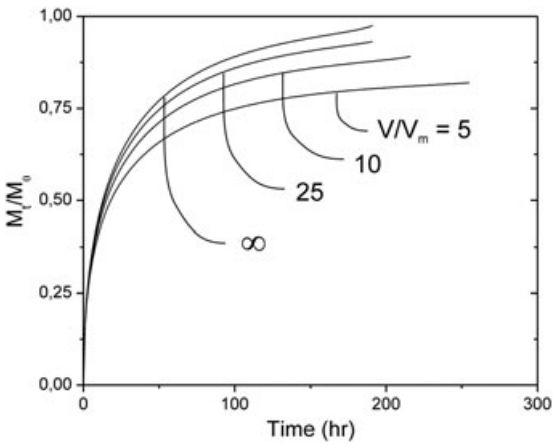

Figure 9. Fraction of drug released calculated according to Equation (19) from a cylindrical matrix into different release medium volume. The parameters used are $R = 0.5$ cm; $h = 3$ cm; $C_S = 0.1$ g/cm^3; $A = 3 \cdot C_3$; $D_p = 1.0 \times 10^{-}6$cm^2/s.

the value for finite volume and multiplied by hundred. The values of Q were divided by C_s and D_p parameters for a more general comparison. Table I can be used in two situations. In a first case, the table can be used to determine the error in the model prediction when sink conditions are assumed instead of taking into account the real value of V used in the experiment. For example, Table I shows that if $V/V_m = 3000$, the error in assuming sink conditions is 0.05%. In a second case, Table I allows to establish the volume of external solution that should be used in the experiment in order to assume sink conditions and to obtain an error according to the accuracy required. For example, if the accuracy required is an error less than 0.01%, the ratio should be set to $V/V_m \geq 15000$. As a result, a decision criterion can be established for the use of the model that takes into account the finite volume. This criterion is based in the percentage error considered as the maximum error in the prediction of the values of amount of drug released. This maximum determinates according to the accuracy required.

A simulation was carried out in order to illustrate the effect of the external medium volume on release. In Figure 9, it can be observed that the straight line covers different time of release, that is because the moving front has reached the center of the device ($S = 0$) at different velocity depending on the volume of external medium. From that moment on, only dissolved drug remains in the device; therefore, the model is not applicable. The amount of dissolved drug remains in the device depends of V/V_m ratio. The higher V/V_m, the greater the *FDR* and therefore the fewer the drugs dissolved remain in the device. In the case of $V/V_m = 5$, the release achieves 82% of the initial amount of drug loaded. In contrast, for $V/V_m = \infty$, the release reaches 98% of the initial drug loaded. This last situation can be explained because of the concentration in the receptor volume remains constant to a small value, which maintains the concentration gradient between the external medium and the matrix in a fixed value. It can also be seen already at short times the curves with finite volume of the external medium begin to show a different behavior to the curve with infinite volume. In these cases, the diffusion begins to compete with the phenomenon of partition between the external environment and the matrix, as the controlling mechanism of the drug release.

The term *sink conditions* were defined differently depending on the author, for example, as 10%, 20% [27], or up to 30% [28] of maximum drug solubility in the external medium to assure that release of drug is not significantly influenced by partition. In other words, it is established that the concentration C_B has a limit to maintain sink conditions. This limit is given by 10%, 20%, or 30% of the maximum concentration of saturation in the external medium of release C_a depending on the criterion chosen. Figure 10 presents a simulation

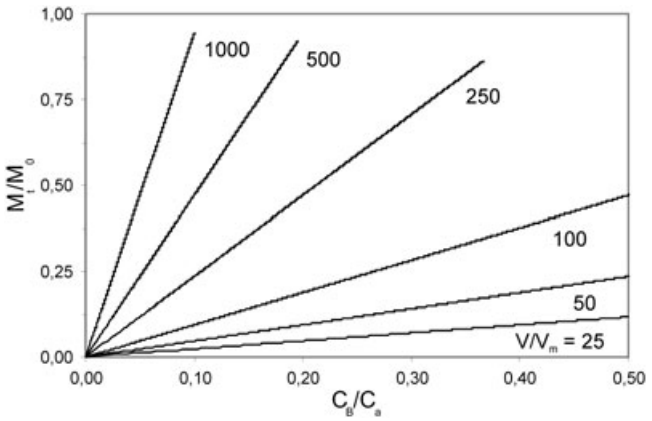

Figure 10. Simulation of fraction of progesterone released versus C_B /C_a ratio from a silicone matrix into a distilled water with different release medium volume. The parameters used are $R = 0.5$ cm; $h = 6$ cm; $C_S = 0.5947$ g/cm^3; $A = 3 \cdot C_3$; $C_a = 0.0168$ mg/cm^3 $D_p = 2.15 \times 10^{-8}$cm^2/s.

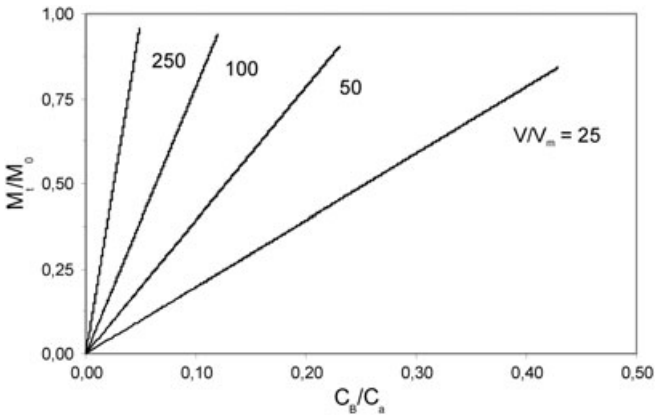

Figure 11. Simulation of fraction of progesterone released versus C_B /C_a ratio from a silicone matrix into a mixture ethanol:distilled water in 20 : 80 ratio, with different release medium volume. The parameters used are $R = 0.5$ cm; $h = 6$ cm; $C_S = 0.5947$ g/cm^3; $A = 3 \cdot C_3$; $C_a = 0.150$ mg/cm^3 $D_p = 2.15 \times 10^{-8}$cm^2/s.

of the release of progesterone, a hydrophobic drug, from a silicone cylindrical device into an external medium of distilled water. The simulation was performed for different external medium volumes of release. The C_S and D_p values were extracted from the literature, see [8]. The maximum solubility of progesterone in distilled water C_a has a low value, approximately 0.0168 mg/cm^3 [29]. The *y*-axis shows the *FDR* at each time *t*, as commonly plotted on release profiles. But the *x*-axis were computed the C_B/C_a ratio, calculated for the entire release process, that is until the moving front, S, reaches the center of the device. The curves obtained show that the increase in the fraction of drug delivered generates an increase in C_B, and therefore, C_B /C_a. If the value of the limit in the C_B /C_a ratio that ensures sink conditions is established in 0.3, the release of progesterone in an external medium with V/V_m =25/50/100/250 generates a release process with two stages. In the first state, there is a diffusion controlled release, because it keeps the sink conditions. In the second stage, there appears the phenomenon of partition, which will begin to influence the release. Fractions of drug delivered to the V/V_m ratio were analyzed in the graphic, beginning the stage controlled by diffusion-partition to 7%, 14%, 28%, and 70%, respectively. If the limit in the C_B /C_a ratio is more strict, for example, 0.1, the drug release continues to show the two stages, to a $V/V_m = 1000$. This means that in this simulated system release a $V/V_m = 1000$ ensures the sink conditions, established as $C_B = 0.1 \bullet C_a$.

Figure 11 shows the same simulation that Figure 10, modifying the composition of external medium, is using in this case the mixture ethanol: distilled water in 20 : 80 ratio. The maximum solubility of progesterone C_a in ethanol 20% in distilled water is 0.15 mg/cm^3 [30]. If the value of the limit in the C_B /C_a ratio that ensures sink conditions is established in 0.3, only the release of progesterone in an external medium with $V/V_m = 25$ generates a release process with two stages. However, if the limit in the C_B /C_a ratio is 0.1, the drug release shows the two stages during the release process, at least up to a $V/V_m = 100$. The release of drug with V/V_m =25/50/100 loses the sink condition when M_t/M_0 reaches to 19%, 39%, and 78%, respectively.

4. Conclusions

Analytical solutions based on the PSSA were derived for the case of controlled dispersed-drug release from IDDS cylindrical matrix type into a finite external medium. The validity of the models was corroborated in two ways. First, the results obtained were compared with the analytical solutions available in the literature for the limiting case where $V \to \infty$. There were differences in values of moving front

and cumulative amount of drug released due to differences in the derivation of the model presented in this work respect to the model reported by Roseman. Secondly, the equations were corroborated by comparison with experimental profiles reported in the literature for finite release medium.The prediction in drug release perfectly fits to the experimental release profiles.

The evolution of concentration distribution profiles as function of the radius of the device for different positions of the diffusion–dissolution moving front was studied. The results showed that by reducing the volume of external solution or the V/V_m ratio, it promotes a greater concentration on the surface of the device, which determines a lower concentration gradient. A decrease in the gradient produces a decrease in both the diffusion moving front velocity as well as in the release of drug. To assume an external concentration equal to zero, it should be established first if the V/V_m of the system allows negligible concentrations in the receiver solution. The definition of decision criterion for the use of the model that takes into account the finite volume has been performed. This criterion is based in the percentage error considered as the maximum error in the prediction of the values of amount of drug released, which depends of accuracy required by the users.

Currently, within the area of IDDS, the investigation of in vitro release systems in finite volume of external solution has a theoretical and practical importance. In this context, the application of the model derived in the present work becomes important.

Acknowledgements

The authors wish to express their gratitude to Consejo Nacional de Investigaciones Científicas y Técnicas (CONICET) and to the Universidad Nacional del Litoral (UNL) of Argentina for the financial support granted to this contribution.

References

1. Segal SJ. *Contraception Research for Today and the Nineties, Part II: Progress in Control Vaccines*, Chapter 4: Steroid Implants for Long-Term Contraception. Progress in Vaccinology. Springer: New York, 1988.
2. Sivin I, Croxatto H, Bahamondes L, Brache V, Alvarez F, Massai R. Two-year performance of a nestorone-releasing contraceptive implant: a three-center study of 300 women. *Contraception* 2004; **69**:137–144.
3. Han Y, Zhang XY, LingLing E, Wang DS, Liu HC. Sustained local delivery of insulin for potential improvement of peri-implant bone formation in diabetes. *Science China Life Science* 2012; **55**:948–957.
4. Gebhardt R, Ludwig M, Kirsner S, Kisling K, Kosturakis AK. Implanted intrathecal drug delivery systems and radiation treatment. *Pain Medicine* 2013; **14**:398–402.
5. Zaki M, Patil SK, Baviskar DT, Jain DK. Implantable drug delivery system: a review. *International Journal of Pharm Tech Research* 2012; **4**:280–292.
6. Collins R. Mathematical modelling of controlled release from implanted drug-impregnated monoliths. *Pharmaceutical Science and Technology Today* 1998; **1**:269–276.
7. Collins R, Paul Z, Reynolds DB, Short RF, Wasuwanich S. Controlled diffusional release of dispersed solute drugs from biodegradable implants of various geometries. *Biomedical Science Instrumentation* 1997; **33**:137–142.
8. Chien YW. Fundamentals of controlled-release drug administration. In *Novel Drug Delivery Systems*, Swarbrick J (ed.). Marcel Dekker Inc.: New York, 1982.
9. Needleman IG. Controlled drug release in periodontics: a review of new therapies. *Britrish Dental Journal* 1991; **170**:405–407.
10. Bourges JL, Bloquel C, Thomas A, Froussart F, Bochot A, Azan F, Gurny R, BenEzra D, Behar-Cohen F. Intraocular implants for extended drug delivery: therapeutic applications. *Advanced Drug Delivery Reviews* 2006; **58**:1182–1202.
11. Peyman GA, Ganiban GJ. Delivery systems for intraocular routes. *Advanced Drug Delivery Reviews* 1995; **16**:107–123.
12. Otsuka M, Matsuda Y, Suwa Y, Fox JL, Higuchi WL. A novel skeletal drug delivery system using a self-setting calcium phosphate cement. 5. Drug release behavior from a heterogeneous drug-loaded cement containing an anticancer drug. *Journal of Pharmaceutical Science* 1994; **83**:1565–1568.
13. Ikegami K, Tagawa K, Kobayashi M, Osawa T. Prediction of in vivo drug release behavior of controlled-release multiple-unit dosage forms in dogs using a flow-through type dissolution test method. *International Journal of Pharmaceutics* 2003; **258**:31–43.
14. Rathbone MJ. Delivering drugs to farmed animals using controlled release science and technology. *International e-Journal of Science, Medicine & Education* 2012; **6**:118–128.
15. Power J, French R, Cowan F. *Subdermal Implantable Contraceptives Versus other Forms of Reversible Contraceptives or other Implants as Effective Methods for Preventing Pregnancy, The Cochrane Collaboration*. John Wiley & Sons: New Jersey, 2008.
16. Roseman TJ, Higuchi WI. Release of medroxyprogesterone acetate from a silicone polymer. *Journal of Pharmaceuticals Science* 1970; **59**:353–357.
17. Zhou Y, Chu JS, Zhou T, Wu XY. Modeling of dispersed-drug release from two-dimensional matrix tablets. *Biomaterials* 2005; **26**:945–952.
18. Zhou Y, Wu XY. Theoretical analyses of dispersed-drug release from planar matrices with a boundary layer in a finite medium. *Journal of Controlled Release* 2002; **84**:1–13.
19. Helbling IM, Ibarra JCD, Luna JA, Cabrera MI, Grau RJA. Modeling of drug delivery from erodible and non-erodible laminated planar devices into a finite external medium. *Journal of Membrane Science* 2010; **350**:10–18.
20. Zhou Y, Wu XY. Modeling and analysis of dispersed-drug release into a finite medium from sphere ensemble. *Journal of Controlled Release* 2003; **90**:23–36.
21. Higuchi T. Rate of release of medicaments from ointment bases containing drug in suspension. *Journal of Pharmaceuticals Sciences* 1961; **50**:874–875.
22. Higuchi T. Mechanism of sustained-action medication. *Journal of Pharmaceuticals Sciences* 1963; **52**:1145–1149.
23. Siegel RA. Theoretical analysis of inward hemispheric release above and below drug solubility. *Journal of Controlled Release* 2000; **69**:109–126.
24. Crank J. *The Mathematics of Diffusion*, 2nd edn. Clarendon Press: Oxford, 1975.
25. Wu XY, Zhou Y. Finite element analysis of diffusional drug release from complex matrix systems. II. Factors influencing release kinetics. *Journal of Controlled Release* 1998; **51**:57–71.
26. Li Y, Xiang Z, Xiang X, Wang S. A computer algorithm for optimizing to extract effective diffusion coefficients of drug delivery from cylinders. *Information Technology Journal* 2010; **9**:1647–1652.

27. FIP Guidelines for dissolution testing of solid oral products. *Joint Committee Report of the Section for Official Laboratories and Medicines Control Services and the Section of Industrial Pharmacists* 1981; **43**:334–343.
28. In-vitro and in-vivo evaluation of dosage forms, 1995. USP 23.
29. Haskins AL. Solubility of progesterone in water and in saline. *Proceedings of the Society for Experimental Biology and Medicine* 1949; **70**:228–229.
30. Bunt CR, Rathbone MJ, Burggraaf S, Ogle CR. Development of a QC release assessment method for a physically large veterinary product containing a highly water insoluble drug and the effect of formulation variables upon release. *International Symposium on Controlled Release of Bioactive Materials* 1997; **24**:145–146.